Citral hydrogenation over Pt loaded micro- and mesoporous supports : the interplay between steric limitations and acidity

CITRAL HYDROGENATION OVER PT LOADED MICRO- AND MESOPOROUS SUPPORTS: THE INTERPLAY BETWEEN STERIC LIMITATIONS AND ACIDITY

Oki Murazaa, Evgeny V. Rebrova, P?ivi M?ki-Arvelab, Narendra Kumarb,Mart H.J.M. de Croona, Jaap C. Schoutena , Dmitry Yu. Murzinb aDepartment of Chemical Engineering and Chemistry, Eindhoven University of Technology, P.O. Box 513, 5600 MB Eindhoven, the N

Abstract

The effect of pore morphology and acidity on the selectivity in the hydrogenation of citral was investigated on a series of bifunctional catalysts: Pt-H-SAPO-5, Pt-H-Y zeolite, and Pt-H-MCM-41. The reaction was studied in a batch reactor at 70◦C with 10 bar total pressure. The highest selectivity to the unsaturated alcohols of 57% was obtained on the Pt-H-SAPO-5 catalyst at a conversion of 46%. The interplay among a monodimensional pore channel of the H-SAPO-5 support, weak Br?nsted acidity of this silicoaluminophosphate, and large platinum nanoparticles contributed to a high selectivity. The corresponding turn over frequency was 0.036 s^{-1}. Pt-H-MCM-41 showed the highest selectivity to menthol as by product, while Pt-H-Y zeolite demonstrated the highest dehydration rate.

Keywords: Citral, H-SAPO-5, Bifunctional catalyst, One-dimensional pore channel

1. Introduction

Unsaturated aliphatic alcohols with an allylic double bond are important reactants in fine chemicals synthesis [1]. They can be obtained by the selective hydrogenation of ?, ?-unsaturated aldehydes which is a rather difficult process as the reaction enthalpy for C=C hydrogenation is by 42 kJ/mol higher than that for C=O hydrogenation [2-4]. The hydrogenation catalysts usually contain noble metals as active components. Pt, Pd, Ni, and Ru monometallic catalysts have often been applied in citral hydrogenation [5, 6]. The selectivity depends strongly on the conditions during catalyst preparation as well as on the nature of the support. Silica [5], titania [6], carbon [7], carbon nanotubes [8, 9], polyanilines [10], zeolites [11], and mesoporous materials [12] have been extensively studied in different structures such as thin films, monoliths, and fibers.

Fig. 1. Citral and its derivatives, formed by C=O hydrogenation, C=C hydrogenation, cyclization, dehydration and double bond migration.

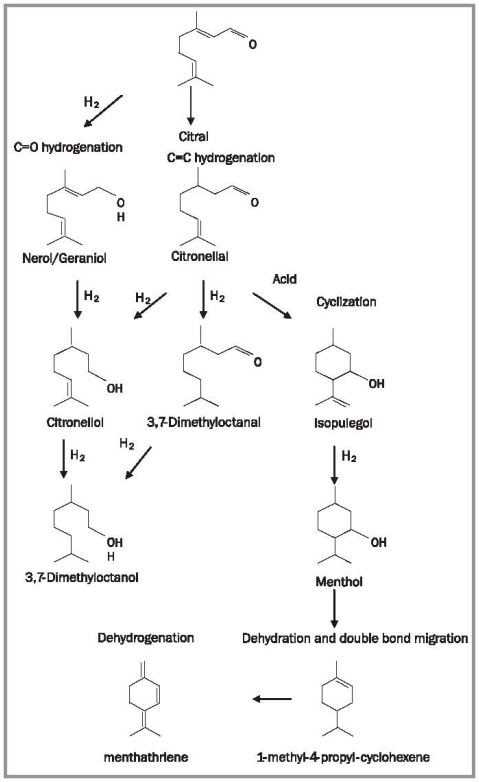

Selective hydrogenation of one of the ?, ?, unsaturated aldehydes, citral (3,7-dimethyl-2,6-octadienal), was chosen in this

study as a model reaction. Citral is usually a mixture of E- and Z-isomers and it can be hydrogenated towards unsaturated aldehyde (citronellal) or unsaturated alcohols (nerol and geraniol). Subsequent hydrogenation of these products leads to citronellol, and then to dimenthyloctanol, while isomerization of citronellal gives isopulegol (IP).

Metal impregnated zeolites can provide shape selectivity in citral and cinnamaldehyde hydrogenation [13, 14]. Comparison with the current work is limited only to literature data on selective hydrogenation of ?, ?, unsaturated aldehydes on microporous zeolites. Other parameters such as bimetallic effect, reducibility of support and other reaction related parameters are beyond the scope of this study. The influence of geometric constraints in the micropores has been demonstrated in the Pt-BEA zeolite, where selectivity to cinnamylalcohol of 88% was reported [4, 14]. To explain the high selectivity, the authors suggested that diffusion of an aldehyde molecule occurred parallel to the linear channel walls until it reached a Pt cluster. This makes the adsorption via a carbonyl group more probable, resulting in selective hydrogenation to the unsaturated aldehyde. A similar effect was observed on a Ru-LTL zeolite catalyst which has a one-dimensional microporous network with a channel diameter of 0.71 nm. A selectivity to nerol and geraniol of 40% was reported at a citral conversion of 60% at 50°C under 50 bar pressure with 2-propanol as a solvent [13].

Aluminum-phosphate-based microporous molecular sieves with a one-dimensional framework structure are other potential candidates for selective hydrogenation of ?, ?-unsaturated aldehydes. The nature of their weak acidic properties has been extensively investigated [15] since their first appearance in the literature [16-18]. H-SAPO-5 has 12-membered rings with an aperture of 0.73 nm in diameter (AFI topology) [19]. On metal-containing H-SAPO-5, the acid as well as the redox properties can be utilized for catalysis. The acidity of H-SAPO-5 can be tuned by changing the Al content resulting in new isomerization routes similar to that reported on Beta and Y zeolites and H-MCM-41 [11, 20].

This paper focuses on the effect of pore morphology and acidity of Pt-H-SAPO-5 and H-SAPO-5 molecular sieves with an AFI structure and their influence on the catalytic performance in citral hydrogenation to unsaturated alcohols (nerol and geraniol). The activity of H-SAPO-5 supported Pt catalyst was investigated and compared with that of Pt-H-Y, and Pt-H-MCM-41, used as reference catalysts. Pt-H-Y exhibits the FAU (faujasite) structure. It has a 3-dimensional pore structure with pores running perpendicular to each other and has a strong acidity. Pt-H-MCM-41 has a one-dimensional framework structure with a weak acidity.

2. Experimental

2.1 Catalyst synthesis

H-SAPO-5 was synthesized according to the procedure by Campelo et al. [21] with several adjustments. The precursors in the synthesis of H-SAPO-5 were phosphoric acid (Merck, 85 wt.%), hydrated aluminium oxide (Vista, 74.2 wt.% Al_2O_3, and 25.8 wt.% H_2O), fumed silica (Aldrich), tri-n-propylamine (Merck), and distilled water. A gel solution was prepared and poured into a Teflon coated stainless steel autoclave and the synthesis was carried out at 473 K for 24 h under static condition [11]. H-MCM-41 was synthesized using fumed silica (Aldrich), tetramethylammonium silicate (Sachem), sodium silicate (Merck), tetradecyl trimethyl ammonium bromide ($CH_3(CH_2)_{13}N(CH_3)_3Br$, Aldrich), and aluminium isopropoxide (Aldrich) by a method described in [22]. H-Y zeolite was obtained by calcination of NH_4-Y (Zeolyst International). The supported platinum catalysts were prepared by impregnation of the corresponding supports with H_2PtCl_6 (40 wt.%, Degussa) in a rotary evaporator for 24 h.

2.2 Catalyst characterization

The acidity of the supports was studied on a ATI Mattson FT-IR spectrometer by pyridine adsorption. A 10 mg/cm² thin tablet of the catalyst was evacuated at 723 K for 1 h. Pyridine (? 99.5 wt.%) was adsorbed at 373 K for 30 min. The desorption was carried out at 473 K. The amount of adsorbed pyridine was calculated based on the molar extinction coefficient [23]. The BET surface area was measured by nitrogen adsorption at 77 K in an ASAP 2010 instrument (Micromeritics). A desired quantity of catalyst powder (1.0 to 5.0 wt.%) was outgassed at 573 K for 4 h prior to the measurements. XRD data were collected on a Rigaku Geigerflex Max/B diffractometer (40 kV, 40 mA) with Cu $K_?$ radiation (using continuous scanning at 0.02o 2 and a counting time of 0.5 s / scan step).

The morphology of the catalysts was determined by transmission electron microscopy (TEM). High resolution transmission electron microscopy (HR-TEM) images/stories/fotki were recorded on a FEI Tecnai TF20 electron microscope operated at 200 kV. The collected powders were grinded and dispersed in ethanol. The suspension was mounted gently to a holey amorphous carbon film on a Ni or Cu grid. The particle size distribution (PSD) was obtained by measuring 100 particles from the TEM micrographs. The mean particle diameter was calculated by the following formula: $d_m = \frac{1}{100}\sum_{i=1}^{100} n_i d_i$, where ni is the number of particles with diameter di.

The dispersion, %D, of the metal nanoparticles was measured by CO pulse chemisorption with stoichiometry 1:1. In case of Pt-H-SAPO-5, the dispersion was estimated from the mean particle diameter obtained from the TEM micrographs by the formula: $\%D = \frac{C_1}{d(nm)}$, where C1 is equal to 108 for supported platinum catalysts [24].

2.3 Catalytic testing

Prior to reaction, the catalysts (300 mg, 1.0-5.0 wt.%)) were reduced in-situ by hydrogen (AGA, 99.999%) at 673 K for 60 min. Then, the reactor, an autoclave (Autoclave Engineers), was cooled to the reaction temperature. A mixture of 0.01 M citral (97 wt.%, Lancaster 5460) in cyclohexane of 200 cm³ was stripped form oxygen and fed to the reactor. The reaction was carried out in the batch mode at 343 K under 10 bar total pressure at a stirring rate of 1500 rpm. Hydrogen was supplied to reach the 10 bar total pressure. Partial pressure of hydrogen in the reactor was 9 bar as calculated from the vapour pressure of cyclohexane at 343 K. Since vigorous stirring and small catalyst particle sizes (< 90 ?m) were applied, the mass transfer resistance could be eliminated [25]. The metal to substrate molar ratio was 20 to 65 in all experiments. Sampling volumes of 1 cm³ were selected for analysis after desired time intervals. The reactants and products were analyzed by a gas chromatograph equipped with a DB-1 capillary column (length: 30 m, internal diameter: 0.25 mm, film thickness: 0.50 ?m). The temperatures of injector and detector were 523 K and 573 K, correspondingly.

3. Results and discussion

3.1. Characterization of the catalysts

The Y zeolite demonstrated the highest concentration of Br?nsted acid sites (Table 1). The acidity of H-MCM-41 and H-SAPO-5 was respectively three and nine time less than that of Y zeolite. The concentration of Lewis acid sites on Y zeolite and H-MCM-41 was considerably higher than that on H-SAPO-5. Introducing metal on the support usually diminishes the number of strongest acid sites [26]. The structure of the micro- and microporous materials, i.e. zeolite Y, H-SAPO-5 and MCM-41 was confirmed by XRD; it remained untagged after Pt loading [27, 28].

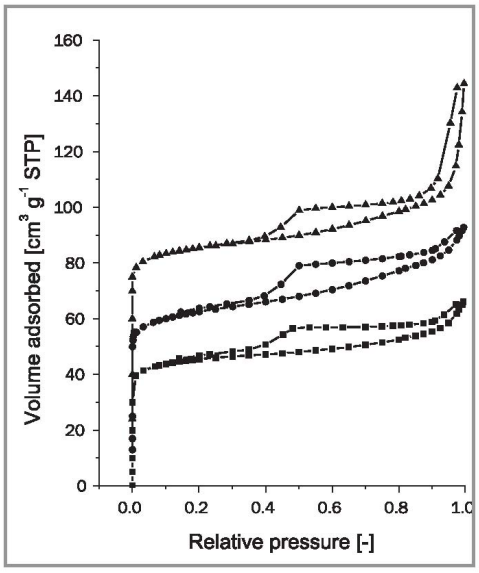

Fig. 2. N2 adsorption-desorption isotherms of H-SAPO-5 (?), Pt-H-SAPO-5, Fresh (?) and Spent (?). Pt-H-SAPO-5, Fresh (?) isotherms were shifted by 10 cm^3/g STP and H-SAPO-5 isotherms were shifted by 20 cm^3/g STP along the Volume Adsorbed axis to obtained well separated isotherms for presentation purposes.

The BET specific surface area of the supports and catalysts are given in Table 1. To be noted, it can be seen that the BET surface area of H-MCM-41 was lower than that of Pt-H-MCM-41, which can be explained by the opening of micropores in the mesoporous material during catalyst preparation; the heat treatment may have opened micropores in the mesoporous material. The specific surface area of the catalysts decreased in the following order: Pt-H-MCM-41 > Pt-H-Y > Pt-H-SAPO-5 (Table 1). The Pt-H-SAPO-5, Pt-H-MCM-41, and Pt-H-Y catalysts have a moderate specific Pt surface area and Pt dispersion in the range of 21 to 29%.

The nitrogen adsorption-desorption isotherms of the H-SAPO-5 support and of the Pt-H-SAPO-5 catalyst are shown in Figure 2.

Table 1. Catalyst characterization data

Catalyst	Acid site concentration of the support (?mol/g_{cat}) a		Specific surface area of the support (m_2/g_{cat})	Specific surface area of the catalyst (m_2/g_{cat})	Support mean pore size (nm)	Pt loading (wt.%)	Specific Pt surface area (m_2/g_{Pt})	Pt dispersion, (%)
	Br?nsted	Lewis						
Pt-H-Y	291	165	1218c	1088 c	0.74	3.8	78	29
Pt-H-MCM-41	89	168	902 b	1189 b	3.0	2.5	67	24
Pt-H-SAPO-5	27	32	220 b	178 b	0.73	1.0	n.d.	21

The initial part of the isotherms corresponds to micropore filling. The subsequent adsorption up to a relative pressure of 0.37 occurs on the outer surface and in the mesopores. An uptake in the adsorption branch of the isotherms in the range of relative pressures between 0.4 and 0.9 corresponds to mesopore filling. Above a relative pressure of 0.9, adsorption takes place mainly on the outer surface and in the macropores which were produced during the pelletizing of the powders [30, 31]. It can be seen that the H-SAPO-5 support has a higher mesopore contribution (0.040 cm^3/g) as compared to the Pt-H-SAPO-5 (0.016 cm^3/g) catalyst. After Pt deposition, the BET surface area decreased from 220 to 178 m^2/g (Table 1). However, the accessibility of the microporous network was not affected by Pt impregnation. The micropore contribution of 124 m^2/g remained unchanged after Pt deposition. The mesopore contribution was considerably reduced from 96 to 54 m^2/g due to partial pore blockage by Pt agglomerates. The Pt-H-SAPO-5 catalyst has a wide distribution of Pt nanoparticles in the range between 2 and 80 nm (Figure 3 (a), (b), and (c)).

The Pt particle sizes can be combined into four groups: 2-4 nm (small), 5-11 nm (medium), 15-20 nm (large), and 50-80 nm (giant).

3.2. Activity of the catalysts

The hydrogenation and the dehydration followed by double bond migration routes in citral transformation (Figure 1) can occur simultaneously and their rates determine the selectivity and the deactivation rate of the catalysts. Dehydration products were typically formed via dehydration of isopulegol or menthol followed by double bond isomerization and thus they consisted of C10 cyclic, unsaturated structures, such as 1-methyl-4-propyl-cyclohexene (Figure 1).

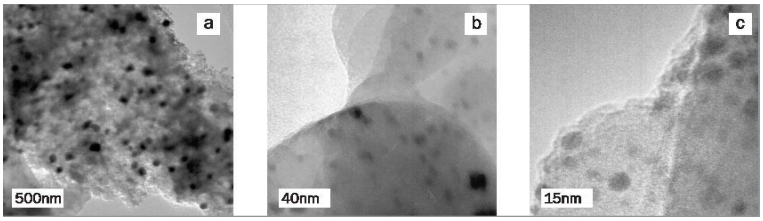

Fig. 3. TEM images/stories/fotki of (a) fresh Pt-H-SAPO-5, (b) magnification of fresh Pt-H-SAPO-5, and (c) spent Pt-H-SAPO-5.

Some of the by-products could also be formed by consecutive dehydrogenation to form menthatriene type compounds which have been confirmed by GC-MS analogously to [11]. The presence of gas-phase low molecular weight hydrocarbons was not analyzed. The adsorption of the dehydration products on the walls of the support porous network leads to fast catalyst deactivation. Therefore, the contribution of each route to the overall conversion of citral was evaluated before a detailed activity study on four types of the supported Pt catalysts was carried out (Figure 4).

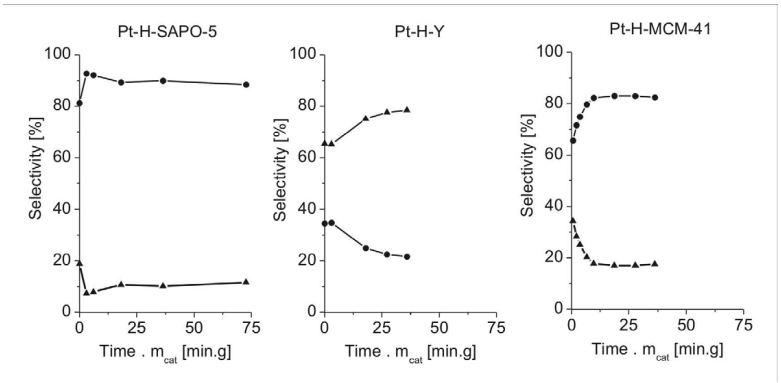

Fig. 4. Selectivity towards hydrogenation (?) and dehydration and double bond migration (?) over Pt-H-SAPO-5, Pt-H-Y, and Pt-H-MCM-41 at 343 K under 10 bar total pressure in cyclohexane. The initial citral concentration was 0.01 M.

The initial hydrogenation and dehydration rates are listed in Table 2. For easier comparison, the selectivity and concentration profiles in Figures 4 to 8 are normalized to 1 gram of Pt. Citral can be strongly adsorbed on the acid sites [11]. It can be seen that the dehydration selectivity is in line with the acidity of the supports. The dehydration and double bond migration dominates over hydrogenation on the Pt-Y catalyst. Its contribution considerably decreases on the Pt-H-MCM-41 and further on the Pt-H-SAPO-5 catalysts. An increase of the dehydration rate with an increase of Br?nsted acidity was also reported over nickel supported H-MCM-41 and H-Y catalysts [11].

Table 2. Kinetic data from citral hydrogenation

Catalyst	TOF (s^{-1})	TOF after 120 min (s^{-1})	Initial overall rate (mmol/min/g_{cat})	Initial reaction rate (mmol/min/g)		Selectivity at 50% conversion (%)		
				Hydrogenation[a] (mmol/min/g_{Pt})	Dehydration (mmol/min/g_{cat})	S_{NG}[b]	S_{CAL}	S_{DH}
Pt-H-Y	0.098	0.016	0.95	8.7	0.62	0	2	67
Pt-H-MCM-41	0.054	0.030	0.20	4.0	0.1	4	10	27
Pt-H-SAPO-5	0.043	0.036	0.11	2.8	0.08	57	4	13

-aHydrogenation rate is presented in mmol/min/gPt unit (not in mmol/min/gcat) as hydrogenation is controlled by the metal nanoparticles.

bwhere CAL is citronellal, NG is nerol + geraniol, and DH = dehydration and double bond migration products.

It is well known that hydrogenation occurs on the metal sites while dehydration occurs on the acid sites. Therefore, the hydrogenation rates below are given per unit of Pt weight while the dehydration rates are calculated per unit of support weight, hereafter.

The turnover frequency (TOF) after a reaction time of 30 min was in the range of 0.02 to 0.07 s^{-1}. The TOF decreased in the following order: Pt-H-SAPO-5, Pt-H-MCM-41 > Pt-H-Y (Table 2). Interestingly the largest TOF was observed for Pt-H-SAPO-5. The pore size of H-MCM-41 was approximately three times higher that of H-SAPO-5 and H-Y. The initial TOF based on initial hydrogenation rate correlates with the size of nanoparticles; e.g. the smaller the particles, the faster hydrogenation rate.

Full citral conversion over Pt-H-Y and Pt-H-MCM-41 was reached within 25 min (Figure 5). However, complete conversion over Pt-SAPO-5 could not be reached within this reaction time due to the fast catalyst deactivation. The BET surface area of the Pt-H-SAPO-5 catalyst decreased from 178 to 154 m^2/g after reaction, mainly due to a decrease in the mesopore surface area from 54 to 36 m^2/g. In other words, about one third of the initial mesopore area was not accessible for nitrogen after the

reaction. The micropore surface area of the spent Pt-H-SAPO-5 catalyst of 118 m^2/g and the micropore volume of 0.054 cm^3/g remained relatively unchanged. The Pt-H-SAPO-5 catalyst after the reaction showed a narrow distribution of predominantly spherical nanoparticles in the range from 5 to 11 nm (Figure 3c). Therefore, neither partial pore blocking nor metal sintering can be responsible for such rapid deactivation. Most probably deactivation is caused by decarbonylation of citral and its hydrogenation products, resulting in strongly adsorbed CO and other carbon fragments [32].

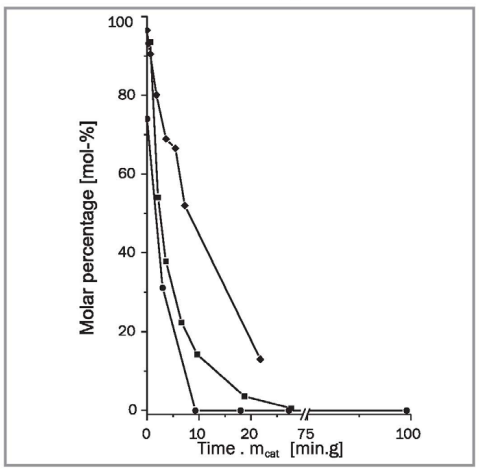

Fig. 5. Citral molar percentage as a function of time over Pt-H-SAPO-5 (?), Pt-H-Y (?), and Pt-H-MCM-41 (?).

Total citral conversion over Pt-H-Y occurred after 10 min with a substantial contribution from the dehydration route. The selectivity to the dehydration products at 50% conversion was 67%. The citral conversion over Pt-H-MCM-41 was 62% after a reaction time of 10 min. Then, the reaction proceeds much slower. The presence of the Br?nsted acid sites was required to achieve high conversion of citral over Ni-H-MCM-41 [11, 33].

Compared with the other micro- and mesoporous support catalysts, activity of Pt-H-SAPO-5 with an H-SAPO-5 support was the highest as shown by the highest TOF and the highest initial hydrogenation rate.

3.3. Selectivity in citral hydrogenation

In citral hydrogenation one of the most important issues regarding catalyst development is to compare chemoselective hydrogenation, i.e. hydrogenation of carbonyl and ethylenic functionalities, respectively. This was performed here in two ways, i.e. by calculating the ratio of the initial rates for formation of nerol and geraniol to that of citronellal , and by reporting selectivities. The ratio between the initial formation rates of nerol and geraniol to citronellal decreased in the following order: Pt-H-SAPO-5 (2.0) > Pt-H-MCM-41 (0.4) > Pt-H-Y (0), indicating that Pt-H-SAPO-5 was five fold more active in the hydrogenation of carbonyl bond than Pt-H-MCM-41, which was the second most active catalyst for hydrogenation of the carbonyl bond. The selectivities towards the main hydrogenation products, nerol and geraniol, citronellal, citronellol, 3,7-dimethyloctanal, 3,7-dimethyloctanol, isopulegol, menthol and towards the dehydration products, are listed in Tables 2 and 3. It should be noted that the sum of the selectivities of the seven main products is often less than 100% due to formation of small amounts of other isomerization by-products, e.g. neomenthol, isomenthol and menthones, which selectivities were not included in further consideration.

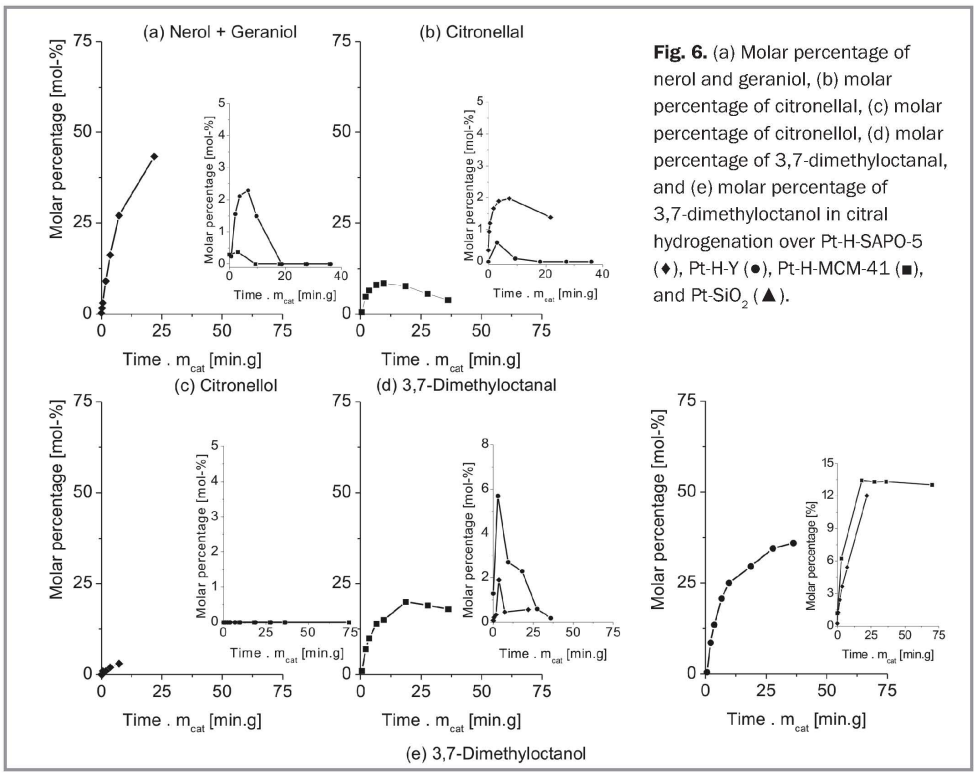

Fig. 6. (a) Molar percentage of nerol and geraniol, (b) molar percentage of citronellal, (c) molar percentage of citronellol, (d) molar percentage of 3,7-dimethyloctanal, and (e) molar percentage of 3,7-dimethyloctanol in citral hydrogenation over Pt-H-SAPO-5 (♦), Pt-H-Y (●), Pt-H-MCM-41 (■), and Pt-SiO_2 (▲).

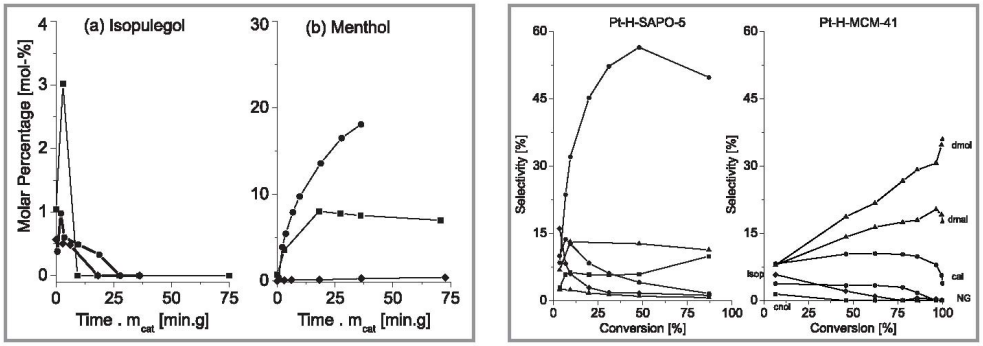

Fig. 7. (a) Molar percentage of isopulegol, and (b) molar percentage of menthol in a 300 min prolonged citral hydrogenation over Pt-H-SAPO-5 (?), Pt-H-Y (?), Pt-H-MCM-41 (?), and Pt-SiO_2 (?).

Comparison of the formation of various products from hydrogenation and cyclisation is depicted in Figures 6 and 7. In the absence of steric limitations and strong acid sites, the supported Pt catalysts are selective in C=C hydrogenation [32]. Hydrogenation of the conjugated C=C bond to citronellal was the main route over Pt-H-MCM-41. The selectivity to the unsaturated alcohols was below 5%. The selectivity towards the undesired dehydration and double bond migration products was 18% over Pt-H-MCM-41 at full conversion of citral.

The most selective catalyst towards nerol and geraniol from the four studied catalysts was the bifunctional Pt-H-SAPO-5, giving nerol and geraniol with a selectivity towards 57% at a citral conversion level of 46% (Table 3). This value was higher than that previously reported on a monodimensional LTL zeolite [13]. The overall kinetics for citral hydrogenation over Pt-H-SAPO-5 is shown in Figure 8a, in which an exceptionally high formation rates for nerol and geraniol compared to those for the citronellal and 3,7-dimethyloctanal generation are clearly visible. Furthermore, citronellol was hydrogenated rapidly to 3,7-dimethyloctanol. An increase of selectivity to the unsaturated alcohols with the increase of citral conversion over Pt-SAPO-5 (Figure 8b) occurred up to about 46% conversion, thereafter selectivity decreased due to consecutive hydrogenation. This curve shape is exceptional, since a typical selectivity curve for a consecutive reaction is similar to that of Pt-H-MCM-41 (Figure 8b), in which the selectivity of an intermediate product started to decrease with increasing conversion. An increasing selectivity to the unsaturated alcohols as a function of conversion has been previously reported for citral [13] and for cinnamaldehyde [34]. This exceptionally selectivity increase on the conversion can be caused by multicentred adsorption where the steric constrains induced by the H-SAPO-5 monodimensional pores influence the number of sites available for adsorption of carbonyl and carbon double bond on Pt-H-SAPO-5 [35].

The steric limitations of the citral molecule with a molecular diameter of 0.58 nm [36] confined in the monodimensional pores of Pt-H-SAPO-5 with a diameter of 0.73 nm, could induce an end-on C=O adsorption mode [14]. As a result, the selectivity to citronellal over Pt-H-SAPO-5 was below 7 % (Figure 9) while a substantial amount of isomerization products (isopulegol) were also produced on the acid sites.

Hydrogenation of the isolated C=C bond rather than of the C=O bond occurred in the second hydrogenation step over Pt-H-MCM-41 catalyst (Figure 6 and Figure 9). As a result, a low selectivity to citronellol and a moderate selectivity to 3,7-dimethyloctanal were observed at larger reaction times. 3,7-dimethyloctanol was formed either via hydrogenation of citronellal or via hydrogenation of nerol and geraniol to citronellol. At longer reaction times, citronellol and 3,7-dimethyloctanal were further hydrogenated on the supported Pt catalysts towards 3,7-dimethyloctanol (Fig. 8a). Thus, if reaction time allows, hydrogenation on the supported Pt catalysts always proceeds towards the fully hydrogenated products in the absence of steric limitations. The highest selectivity to 3,7-dimethyloctanol of 34% was observed on the micro(meso)porous Pt-H-MCM-41 catalyst. It is also possible to stop the reaction after the second hydrogenation step (citronellol) using Ni as an active metal [37, 38].

However, not all citral was hydrogenated towards citronellol over the bifunctional Pt-H-MCM-41 and Pt-H-Y catalysts. The product of the first hydrogenation step, citronellal, was isomerized to isopulegol on the acid sites and further hydrogenated to menthol (Figure 7b) at longer reaction times [38-41]. Pt-H-MCM-41 catalyst was the most selective one to menthol with 18% selectivity at a citral conversion of 25% (Table 3). Unlike Ni-H-MCM-41, platinum supported H-MCM-41 was less selective to cyclization route and menthol at long reaction times [12] due to the fast subsequent hydrogenation of citronellol to 3,7-dimethyloctanol. The most acidic catalyst (Pt-H-Y) was also not selective in cyclization route due to considerable conversion of citral towards dehydration products (e.g. menthatrienes) which were the main products with a selectivity of 67% at full citral conversion (Table 2). The highest selectivity to menthol was 7%. The selectivity to isopulegol over the Pt-H-SAPO-5 catalyst was below 2%.

4. Conclusions

Hydrogenation of citral was investigated on a series of bifunctional catalysts: Pt-H-Y zeolite, Pt-SAPO-5, as well as on a supported Pt-MCM-41 catalyst. The initial reaction rate in terms of TOF was the highest on the mesoporous Pt-H-MCM-41 catalyst, followed by the microporous Pt-H-SAPO-5, and finally the microporous Pt-H-Y. The acid site concentration decreased in the reversed order. In this way, the H-Y support showed the highest activity in dehydration and double bond migration, which was due to its highest concentration of Br?nsted acid sites. H-SAPO-5 was the most selective support for hydrogenation towards the unsaturated alcohols with selectivity of 57% at the conversion level of 46%. A unique combination of a monosized pore diameter, weak Br?nsted acidity, and a large Pt particle size contributed to a high selectivity. However, rapid deactivation occurred on this support due to adsorption of the dehydration products and partial pore blocking. Pt-H-MCM-41 was the most selective catalyst for the formation of menthol. However, on this catalyst, the parallel dehydrogenation reaction still consumed 18% of citral, while the deactivation rate was less pronounced as compared with H-SAPO-5. Further reducing the size of platinum nanoparticles is required to fully explore the benefit of using unidimensional pore of microporous zeolites such as H-SAPO-5 in selective hydrogenation.

Acknowledgements

The financial support by the Dutch Technology Foundation (STW, project no. EPC.6359), Shell, Akzo Nobel Chemicals, Schering-Plough, DSM, Bronkhorst, TNO, and the Finnish Centre of Excellence Programme (2000–2011) of the Academy of Finland are gratefully acknowledged. Authors are grateful to Mr. Markku Reunanen for MS analysis at ?bo Akademi University and Dr. Ugo Lafont from Delft University of Technology for the TEM measurements.

Fig. 6. (a) Molar percentage of nerol and geraniol, (b) molar percentage of citronellal, (c) molar percentage of citronellol, (d) molar percentage of 3,7-dimethyloctanal, and (e) molar percentage of 3,7-dimethyloctanol in citral hydrogenation over Pt-H-SAPO-5 (?), Pt-H-Y (?), Pt-H-MCM-41 (?), and Pt-SiO_2 (?).

Fig. 9. Selectivity of main citral derivatives as a function of conversion over a) Pt-H-SAPO-5 and b) Pt-H-MCM-41: nerol and geraniol (?), citronellal (O), citronellol (?), 3-7, dimethyloctanal (?), and 3-7, dimethyloctanol (?).

Table 3. Selectivity of selected main products in citral hydrogenation over Pt-H-SAPO-5 and Pt-H-MCM-41 catalysts

Catalyst	X_{citral} [a] [-]	CAL	NG	COL	DMAL	DMOL	IP	MT	?
Pt-H-SAPO-5	25	7	48	6	2	13	2	6	84
	46	4	57	6	1	13	2	3	82
	75	2	52	9	1	12	1	3	80
	87b	2	50	10	1	11	1	3	78
Pt-H-MCM-41	25	9	4		11	13	4	18	60
	50	10	4	-	15	19	2	14	63
	75	10	3	-	17	26	1	15	72
	99	6	-	-	19	34	1	23	83

[a]where X is conversion, CAL = citronellal, NG = nerol + geraniol, COL = citronellol, DMAL = 3,7-dimethyloctanal, DMOL = 3,7-dimethyloctanol, IP = isopulegol, and MT = menthol. ? is the total selectivity for the main products excluding other menthols such as isomenthol and neomenthol.

bthe experiment was carried out until conversion of 87%.

References

1. Surburg H., Panten J., Common Fragrance and Flavor Materials: Preparation, Properties and Uses, 5th Ed., Wiley-VCH,

Berlin, 2006.

2. Creyghton E.J., Downing R.S., J. Mol. Catal. A: Chem. 1998. V. 134. P. 47.

3. M?ki-Arvela P., Hajek J., Salmi T., Murzin D. Yu., Appl. Catal A: Gen, 2005. V. 292. P. 1.

4. Claus P., Top. Catal. 1988. V. 5. P. 51.

5. (a) Singh U.K., Vannice M.A., J. Catal. 2000. V. 191. P. 165. (b) Singh U.K., Sysak M.N., Vannice M.A., J. Catal. 2000. V. 191. P. 181. (c) Singh U.K., Vannice M.A.,

J. Catal. 2001. V. 199. P. 73.

6. Malathi R., Viswanath R. P., Appl. Catal. A: Gen. 2001.

V. 208. P. 323.

7. Galvagno S., Milone C., Donato A., Neri G., Pietropaolo R., Catal. Lett. 1993. V. 18. P. 349.

8. Asedegba-Nieto E., Guerrero-Ruiz A., Rodr?guez-Ramos I., Carbon 2006.V.44.P.799.

9. Guo G., Qin F., Yang D., Wang C., Xu H., Yang S., Chem. Mater. 2008. V. 20. P. 2291.

10. Steffan M., Klasovsky F., Arras J., Roth C., Radnik J., Hofmeister H., Claus P., Adv. Synth. Catal. 2008. V. 350. P. 1337.

11. M?ki-Arvela P., Kumar N., Kubi?ka D., Nasir A., Heikkil? T., Lehto V-P., Sj?holm R., Salmi T., Murzin D. Yu., J. Mol. Catal. A: Chem. 2005. V. 240. P. 72.

12. Guisnet M., Guidotti M., One-pot Reactions on Bifunctional Catalysts, in Catalysts for Fine Chemical Synthesis, Microporous and Mesoporous Solid Catalysts, Vol. 4, E.G. Derouane (Ed.), pp. 165-166, John Wiley & Sons, Chichester (2006).

13. (a) Alvarez-Rodriquez J., Guerrero-Ruiz A., Rodriguez-Ramoz I., Arcoya A., Micropor. Mesopor. Mater. 2008. V. 110. P. 186. (b) ?lvarez-Rodr?guez

J., Guerrero-Ruiz A., Rodr?guez-Ramos I., Arcoya-Mart?n A., Catal. Today. 2005. V. 107-108. P. 302.

14. Gallezot P., Blanc B., Barthomeuf D., Pa?s da Silva M.I. Stud. Surf. Sci. Catal. 1994. V. 84. P. 1433.

15. Parlitz B., Schreier E., Zubowa H.L., Eckelt R., Lieske E., Lischke G., Fricke R. J. Catal. 1995. V. 155. P. 1.

16. Lok B.M., Messina C.A., Patton R.L., Gajek R.T., Cannan T.R., Flanigen E.M., US Patent No. 4 440 871, 1984.

17. Wilson S.T., E.M. Flanigen E.M., US Patent

No. 4 567 029, 1986.

18. Lok B.M., Messina C.A., Patton R. L., Gajek R.T., Cannan T.R., Flanigen E.M., J. Am. Chem. Soc. 1984. V. 106. P. 6092.

19. Meier W. M., Olson D.H., Baerlocher Ch., in Atlas of Zeolite Structure Types, Elsevier, Amsterdam, 4th Ed., 1996.

20. Martens J.A., Janssens C., Grobet P.J., Beyer H.K., Jacobs P.A., In: P.A. Jacobs, R.A. Van Santen, Eds., Zeolites: Facts, Figures, Future, Stud. Surf. Sci. Catal. 1989. V. 49A. P. 215.

21. Campelo J.M., Lafont F., Marinas J.M., J. Catal. 1995.

V. 156. P. 11.

22. Beck J.S., Vartuli J.C., Roth W.J., Leonowicz M.E., Kresge C.T.,Schmitt K.D., Chu C.T., Olson D.H., Sheppard E.W., McCullen S.B.,Higgins J.B., Schlenker J.L., J. Am. Chem. Soc. 1992.

V. 114. P. 10834.

23. Emeis C.A., J. Catal. 1993. V. 141. P. 347.

24. Bartholomew C.H., Farrauto R.J., Fundamentals of Industrial Catalytic Processes, 2nd Ed., John Wiley, 2006.

25. Van Santen R.A., Van Leeuwen P.W.M.N., Moulijn J.A., Averlill B.A., Eds. Catalysis: An Integrated Approach, 2nd Ed., Stud. Surf.Sci. Catal. 123, Elsevier, Amsterdam. 1999, P. 375.

26. Kubi?ka D., Kumar N., Ven?l?inen T., Karhu H., Kubickova I., Murzin D. Yu., J. Phys. Chem. B, 2006. V. 110. P. 4937.

27. Kubi?ka D., Kumar N., M?ki-Arvela P., Ven?l?inen T., Tiitta M., Salmi T., Murzin D. Yu., Stud. Surf. Sci. Catal., 2005. V.

158B. P. 1669.

28. Toukoniitty E., ?ev??kov? B., Kumar N., M?ki-Arvela P., Salm T. i, V?yrynen J., Ollonqvist T., Kooyman P., Stud. Surf. Sci. Catal., 2000. V. 135. 23-P-15.

29. M?ki-Arvela P., Kumar N., Paseka I., Salmi T., Murzin D. Yu., Catal. Lett. 2004. V. 98. P. 173.

30. Boddenberg B., Rani V.R., Grosse R., Langmuir. 2004. V. 20. P. 10962.

31. Sing K.S.W., Everett D.H., Haul R.A.W., Moscou L., Pierotti R.A., Rouquerol J., Siemieniewska T., Pure Appl. Chem. 1985. V. 57. P. 603.

32. Burgener M., Wirz R., Malat T., Baiker A., J. Catal. 2004. V. 228. P. 152.

33. Mertens P.G.N., Verpoort F., Parvulescu A-N., De Vos D.E., J. Catal. 2006. V. 243. P.7.

34. Hajek J., Kumar N., M?ki-Arvela P., Salmi T., Murzin D.Yu.,Paseka I., Heikkil? T., Laine E., Laukkanen P. and V?yrynen J.,Appl. Catal. A: Gen. 2003. V. 251. P. 385.

35. Murzin D.Yu., Backman H., React. Kinet. Catal. Lett. 2007. V. 91. P. 141.

36. Mukherjee S., Vannice M.A., J. Catal. 2006. V. 243. P. 108.

37. M?ki-Arvela P., Tiainen L.-P., Lindblad M., Demirkan K., Kumar N., Sj?holm R., Ollonqvist T., V?yrynen J., Salmi T., Murzin D.Yu.,Appl. Catal. A: Gen. 2003. V. 241. P. 271.

38. M?ki-Arvela P., Kumar N., Nieminen V., Sj?holm R., Salmi T., Murzin D.Yu., J. Catal. 2004. V. 225. P. 155.

39. Chuah G.K., Liu S.H., Jaenicke S., Harrison L.J., J. Catal. 20. V. 200. P. 352.

40. Milone C., Gangemi C., Neri G., Pistone A. and Galvagno S., Appl. Catal. A: Gen. 2000. V. 199. P. 239.

41. (a) Trasarti A.F., Marchi A.J., Apesteguia C.R., J. Catal. 2004. V. 224. P. 484. (b) Trasarti A.F., Marchi A.J., Apesteguia C.R., J. Catal. 2007. V. 247. P. 155.